Application of Adaptive Neurofuzzy Inference System for calculation of heat power consumption using infrared thermography

Sebastian Dudzik, Waldemar Minkina,
Częstochowa University of Technology, Institute of Electronics and Control Systems
Al. Armii Krajowej 17, 42-200 Częstochowa, POLAND
e-mail: sebdud@el.pcz.czest.pl, minkina@el.pcz.czest.pl

1. Introduction

In this paper a new method for calculation of heat power consumption in a heat exchanger is described. The method is based on the analysis of phenomena occurring on the ambient side. The calculation of heat power consumption represents an inverse heat transfer problem [1, 2]. In [3] an artificial neural network was used to approximate the characteristics of a heat exchanger. In this paper an Adaptive Neurofuzzy Inference System (ANFIS), trained with data obtaining from infrared thermography measurements [4, 5, 6, 7, 8] is used to calculate the heat power consumption in steady state. The experiments were carried out using measuring stand with an open chamber [9].

The problem of calculation of heat power consumption on the basis of the temperature distribution on the front surface of a radiator can be considered as the convective-radiative, inverse problem [1, 2]. In the typical (simple) heat transfer problem, the heat flux or fluid temperature is usually known. In the convective-radiative inverse problem, the temperature distribution on the considered surface is known. In this case, fluid parameters or the heat flux are investigated [10, 11].

2. Experimental investigations

2.1 Procedure of obtaining the input data

The process of obtaining the data for the artificial neural network can be divided into the following stages [3]:

1. Recording of the thermograms of the investigated radiator on the measured stand with the open chamber in steady state.
2. Averaging of the thermogram series and making of the differential thermogram.
3. Making of the input data sets according to assumed variant of the input data selection with the sofisticated software (on the basis of the differential thermogram).

In the considered heat transfer process, the most important role plays the temperature difference occurring between the radiator surface and the ambient [2, 14]. Furthermore, in the non-isothermal surface case, the temperature distribution of this surface is required. In this paper the differential thermogram was used as the input data source. During the experimental research, the series of 60 thermograms of the front surface of the radiator was recorded. Then, the averaging of all the thermograms for each pixels was made. The averaging was made using the following formula [3]:

$$\bar{t}(x, y) = \frac{1}{60}\sum_{i=1}^{60} t_i(x, y), \tag{1}$$

where: $\bar{t}(x, y)$ – averaged temperature for the *(x, y)* pixel coordinates in the thermogram plane (°C), $t_i(x, y)$ – temperature of *i-th* pixel value in the thermogram plane (°C).

Besides of the recording of the temperature distribution, the reference ambient temperature was measured as well. The reference ambient temperature denotes the air temperature in the central axis of the exploratory chamber, across from the investigated radiator, on the height of (0,75 ± 0,001) m above the floor, in accordance with the recommendation of the DIN 4704-2 standard. The differential thermogram was made by subtracting the reference ambient temperature from each of the thermogram pixels. It was done by following formula:

$$t_{\Delta}(x, y) = \bar{t}(x, y) - t_r, \tag{2}$$

where: $t_{\Delta}(x, y)$ – the temperature for the *(x, y)* pixel coordinates in the differential thermogram plane (°C), t_r – the reference ambient temperature (°C).

The radiator under consideration was investigated in the different inflow temperatures t_1 of the supplied water. Furthermore the volumetric flow of the water was adjusted as well. The differential thermograms, obtained for three exemplary inflow temperatures t_1 and volumetric flow q_v equal to 86 l/h, were presented in Fig. 1, 2.

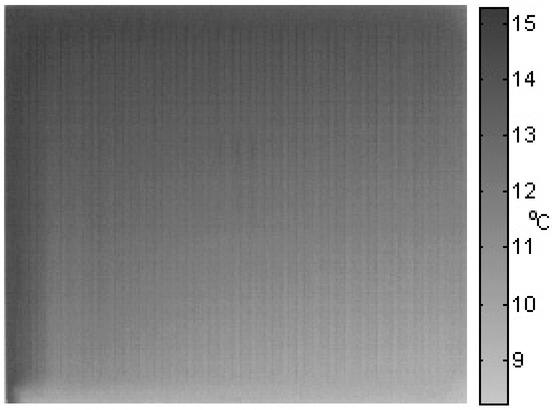

Fig. 1. Differential thermogram for t_1 = 40 °C and q_v = 86 l/h

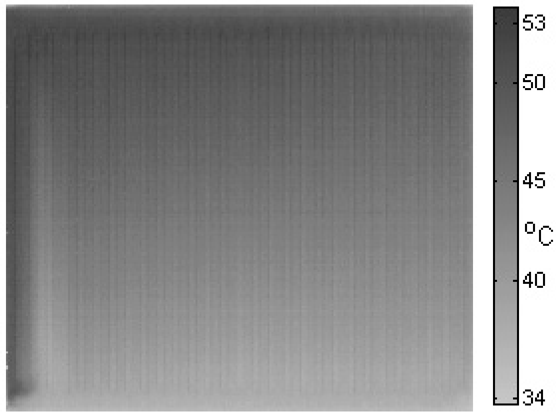

Fig. 2. Differential thermogram for t_1 = 80 °C and q_v = 86 l/h

3. Simulation Research

3.1 Algorithm for calculation of heat power consumption using ANFIS

The solution of coefficient inverse heat conduction problems was presented e. g. in [12, 13]. In this paper, an artificial neural network is used to calculate the heat power consumption of a radiator in a central heating system. The input data for adjusting the ANFIS parameters were obtained from thermograms of considered radiator surface. The output data (measured heat power consumption) were obtained using the measuring stage with open chamber equipped with a PC and suitable measurement instruments. Ambient temperature was also measured using the stage described above. The proposed algorithm for calculation of heat power consumption operates in the two following modes:

1. Tuning mode. In this mode, data obtained from differential thermograms are applied to the inputs of the fuzzy neural network. The heat power consumption is applied to the output of the fuzzy neural network. Additionally, adaptation of the parameters of the input and output membership functions and parameters of the fuzzy rules' set is performed. It is done using a hybrid learning algorithm.
2. Reconstruction mode. In this mode the data obtained from the on-line recorded thermograms are applied to the inputs of the ANFIS. Taking into account the fuzzyfication, inference and defuzzyfication stages, the approximated heat power consumption of the investigated radiator is calculated as the result of the algorithm.

The ANFIS, carries out the algorithm is shown in Fig. 1.

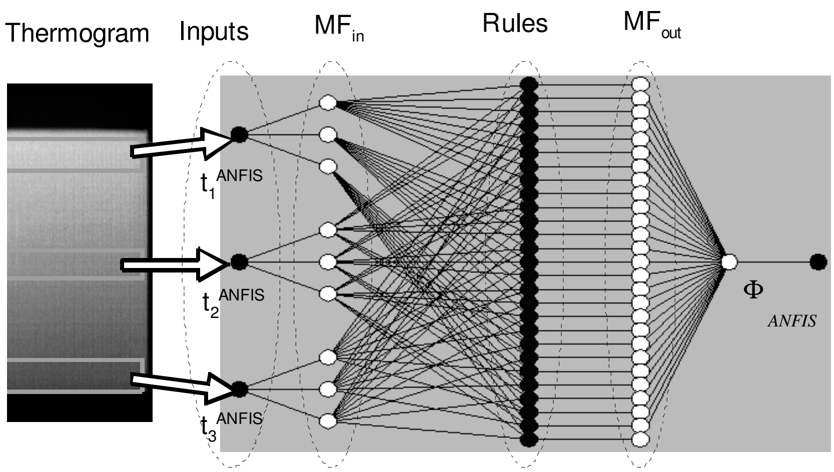

Figure 3. Diagram of the algorithm for calculation of heat power consumption using ANFIS

3.2 Variants of the input data selection

During the simulations of the algorithm for calculation of the heat power consumption, the criteria of the input data selection were assumed. For definition of the input data selection variants, the followed assumptions were made:

- Accessibility of the function carrying out the chosen parameter determination (e. g. average temperature for the area, temperature profiles) in the infrared system.
- Possibility of application of the described algorithm in the measurement systems without infrared camera (e. g. temperature measurement made using contact methods)

In this paper the following variants of the input data selection were assumed:

1. The difference between the averaged temperature from one control area (in the form of the square about 10x10 pixels) and the reference ambient temperature – single-input neural network – Fig. 4.
2. The difference between the averaged temperature from two control areas (in the form of the square about 10x10 pixels) and the reference ambient temperature – two-input neural network – Fig. 5.
3. The difference between the averaged temperature from the three control areas (in the form of the square 10x10 pixels) and the reference ambient temperature – three-input neural network – Fig. 6.

The locations of the control areas were presented in the Fig 4-6 [3].

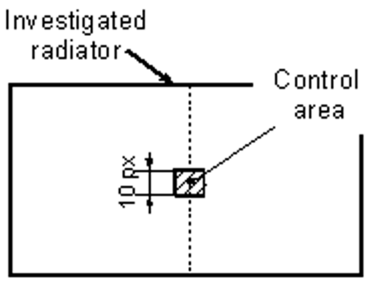

Fig. 4. Location of the control area in the first variant of input data selection

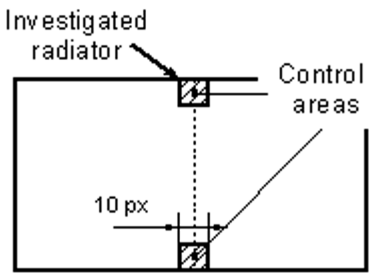

Fig. 5. Locations of the control areas in the second variant of input data selection

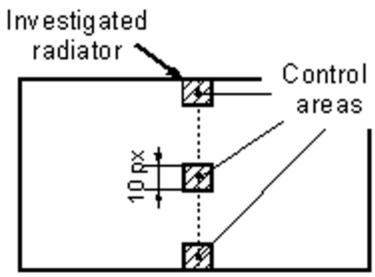

Fig. 6. Locations of the control areas in the third variant of input data selection

4. Results

In this paper, the results of the research for the third variant of input data selection are presented. Due to the influence of the initial conditions on the simulation results, 20 simulations were carried out in this work. The results were averaged. The following criteria of the approximation accuracy were assumed:

– the relative error of the algorithm for a single sample:

$$\delta_{ANFIS} = \frac{\Phi_{ANFIS} - \Phi_{MES}}{\Phi_{MES}} \ (\%), \tag{3}$$

where: Φ_{ANFIS} – value of the heat power consumption, on the output of the ANFIS algorithm (W); Φ_{MES} – value of the heat power consumption measured in the experimental research (W),

– the limiting relative error of the algorithm for all the measured data:

$$\widehat{\delta}_{ANFIS} = MAX\{\delta_{ANFIS}\} \ (\%). \tag{4}$$

– the limiting error of the algorithm within the range of the standard characteristic:

$$\widehat{\delta}^{norm}_{ANFIS} = MAX\{\delta^{norm}_{ANFIS}\} \ (\%), \tag{5}$$

where: δ^{norm}_{ANFIS} - relative error for each sample within the range of the standard characteristic.

The standard characteristic of the investigated radiator was obtained on the measuring stand with the closed chamber. It was done in order to calibrate of the method. The analysis of results was performed for three kinds of membership functions: Gauss, trapezoidal and triangular. They were assumed two kinds of output functions: constant and linear. In simulations the number of input membership functions was changed. The results of fuzzyfication of input variable for different number and shapes of membership functions are presented in Fig. 7, 8.

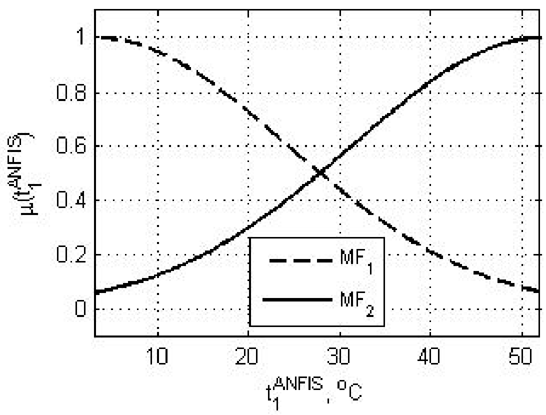

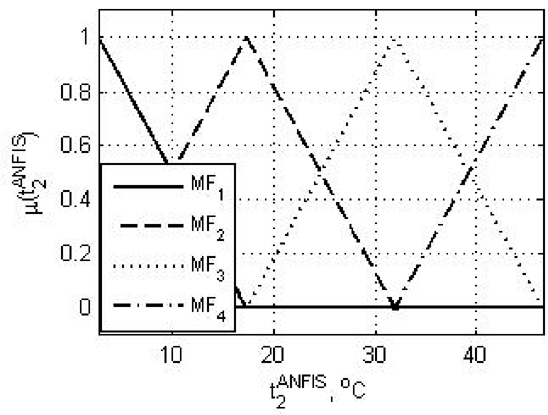

Fig. 7. Two Gaussian membership functions of input variable

Fig. 8. Four triangular membership functions of input variable

In Fig. 9-12, the exemplary results of the simulations of the described algorithm are presented. In simulations it was assumed two and three input membership functions of triangular type. The output membership functions were constant and linear.

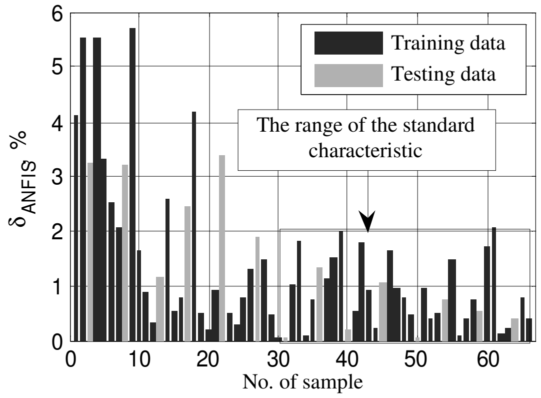

Fig. 9. The relative ANFIS errors: two triangular membership function of inputs, constant membership function of output

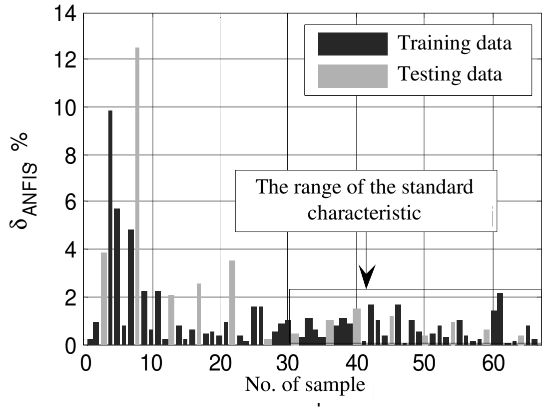

Fig. 10. The relative ANFIS errors: two triangular membership function of inputs, linear membership function of output

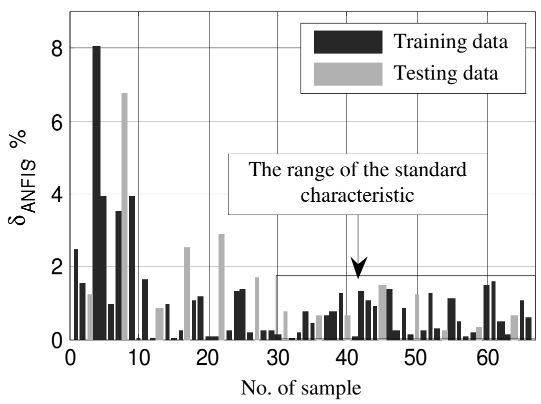

Fig. 11. The relative ANFIS errors: three triangular membership function of inputs, constant membership function of output

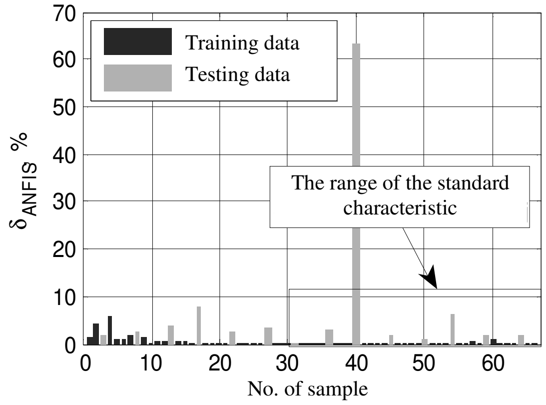

Fig. 12. The relative ANFIS errors: three triangular membership function of inputs, linear membership function of output

In Table 1 it was collected the relative errors values of ANFIS algorithm for constant membership function of output. Triangular membership functions of inputs were assumed.

The number of membership functions of input			$\hat{\delta}_{ANFIS}$ (%)	δ_{ANFIS} (%)	$\hat{\delta}^{norm}_{ANFIS}$ (%)	δ^{norm}_{ANFIS} (%)
t_1^{ANFIS}	t_2^{ANFIS}	t_3^{ANFIS}				
2	2	2	5,8	1,4	2,0	0,8
3	4	3	8,0	1,1	1,6	0,7
5	5	5	7,8	1,0	8,0	0,7

Table 1. The relative errors of ANFIS algorithm with assumption of triangular membership functions of inputs and constant membership function of output.

5. Conclusions

On the basis of the presented simulation results the following conclusions can be formulated:

- The application of the ANFIS algorithm, trained with data obtained from infrared thermography, enables determination of heat power consumption of investigated radiator in a steady state.
- The relative error of determination the heat power consumption by means ANFIS algorithm is minimized in the range of the standard characteristic of investigated radiator.
- The absolute value of ANFIS relative error not exceeds 2%, if the measured heat power consumption contains in the range of the standard characteristic – Fig. 9-12.
- The values of the ANFIS limiting relative errors strongly depend from the numbers and shapes of the inputs' and outputs' membership functions as well.
- The smallest value of the ANFIS limiting relative error was obtained for the triangular membership functions of inputs – table 1.
- The best case from the point of view of the ANFIS algorithm accuracy is the following: three triangular membership functions of t_1^{ANFIS} (input 1), t_3^{ANFIS} (input 3) and four triangular membership functions of t_2^{ANFIS} (input 2) – Table 1.

References

[1] Beck J. V., Blackwell B., Clair JR, Ch. R. St.: „Inverse heat conduction", John Wiley & Sons Inc., New York 1985.

[2] Kreith F.: „The CRC Handbook of Thermal Engineering", CRC Press LLC, 2000.

[3] Dudzik S.: „Calculation of the heat power consumption in the heat exchanger using artificial neural network", 9th International Conference on Quantitative Infrared Thermography, Kraków, July 2–5, 2008, pp. 55–60.

[4] Minkina W., Dudzik S.: „Simulation analysis of uncertainty of infrared camera measurement and processing path", Measurement – Vol. 39, Issue 8, pp. 758-763, Elsevier Ltd, 2006.

[5] Minkina W., Dudzik S. "Infrared Thermography: Errors and Uncertainties", John Wiley & Sons – in print.

[6] Astarita T., Cardone G., Carlomagno G.M., Meola C.: „A survey on infrared thermography for convective heat transfer measurements", Optics & Laser Technology, Vol. 32 (2000) pp. 593-610, Elsevier Science Ltd, 2000.

[7] Minkina W.: "Thermovision Measurements – Methods and Instruments", Technical University of Czestochowa Publishers, Czestochowa 2004, ISBN 83-7193-237-5.

[8] Bąbka R., Minkina W.: „Sub-pixel edge location in thermal images using a meansquare measure" 7th International Conference on Infrared Sensors & Systems (IRS^{2}'2002), 14-16.05.2002, Erfurt, RFN, pp. 213-218.

[9] DIN 4704-2: „Prüfung von Raumheizkörpern, Offene Prüfkabine", 1998.

[10] Özisik M.N.: "Radiative transfer and interactions with conduction and convection", John Wiley & Sons, New York 1973.

[11] Islamoglu Y.: "A new approach for the prediction of the heat transfer rate of the wire-on-tube type heat exchanger–use of an artificial neural network model", Applied Thermal Engineering Vol. 23 (2003), pp. 243-249, Elsevier Science Ltd., 2003.

[12] Nelles O.: „Nonlinear System Identification. From classical Approaches to Neural Networks and Fuzzy Models", Springer-Verlag, Heidelberg, 2001.

[13] Li H., Chen C. L. P.: „Fuzzy Neural Intelligent Systems. Mathematical Foundation and the Applications in Engineering", CRC Press LLC, 2001.